Polymer Brushes Formed by End-Capped Poly(ethylene oxide) (PEO) at the Air−Water Interface

C. Barentin, P. Muller,* and J. F. Joanny

Institut Charles Sadron, 6 rue Boussingault, 67083 Strasbourg Cedex, France

Received November 12, 1997

ABSTRACT: We study monolayers formed at an air−water interface on a Langmuir trough by telechelic poly(ethylene oxide) polymers end capped with hydrophobic alkane groups (C_{12} and C_{16}). The pressure−area isotherms show two plateaus: the first plateau at low coverage already exists for nontelechelic PEO and is attributed to the formation of loops in the solution; after this plateau, the pressure rises stongly as the hydrophobic groups anchor the polymers on the surface, which leads to the formation of a grafted polymer layer; the second plateau at high density is due to a dissolution of the polymer chains in the bulk water. Starting from a monolayer at high density, we also study experimentally the relaxation of the surface pressure with time due to the dissolution of the polymer. A theoretical approach of this problem based on polymer brush theory is proposed. Both the static properties of the layer and the desorption kinetics are calculated. The model accounts well for the shape of the isotherms and for the relaxation kinetics. It gives a good interpretation of the role of various parameters such as the compression velocity, the molecular weight, and the hydrophobicity of the chain ends. The anchoring energy of the hydrophobic groups is determined by comparison with experiments.

1. Introduction

When polymer chains are grafted by one or two of their end points on a surface, the excluded volume interactions between neighboring chains are strong and the chains are stretched toward the solution. If the grafting density is high enough, a dense and thick polymer layer is formed, which has been often called a polymer brush. Polymer brushes are attractive candidates for many technical applications such as the stabilization[1] of colloidal particules that would aggregate in the absence of polymers or lubrication.[2] However, because of the very high energy barrier due to the excluded volume interactions with the chains already forming the brush, it is difficult to incorporate new chains in the brush and thus to form very dense brushes. One way to form brushes is to use a block copolymer (diblock or triblock) where one of the sequences is strongly adsorbed on the interface and anchors another block that is highly soluble. A less extreme case is obtained by attaching small hydrophobic groups to a water soluble polymer and thus to try to form polymer brushes with a so-called telechelic associating polymer in solution in water. In this paper, we study grafted polymer layers formed by poly(ethylene oxide) molecules that have been end capped at both chain ends by small alkane segments (C_{12} and C_{16}). These polymers have been extensively studied in the bulk,[3] where they show a strong associating behavior, the hydrophobic groups forming well-defined aggregates that lead to the formation of a physical gel at high enough concentration. They are also good potential candidates for stabilizing solid dispersions in water.

The formation of a polymer brush at the air−water interface is studied here by spreading the end-capped PEO on a Langmuir trough. The grafting density, i.e., the number of chains per unit area, is varied by adjusting the total area of the monolayer. We thus measure the pressure isotherms of the polymer monolayer. At high pressures, however, the chains are highly stretched and eventually some of the chains dissolve in water due the high solubility of the PEO polymer, to relax the stretching. The pressure then decays with time. We are mostly interested here in the relaxation of dense monolayers and in the desorption kinetics of the grafted chains from the monolayer toward the free solvent (water). The pressure−area isotherms of PEO end capped by $C_{16}H_{33}$ were studied by Kim and Cao.[4] They found that end-capped PEO polymers have an additional surface pressure increase at high density compared to pure PEO monolayers. They also showed that this increase is roughly proportional to the polymer density, as opposed to the low-density part where the pressure is proportional to the monomer density. These results were interpreted as a change in the affinity of the PEO monomers for the solvent molecules as the monomer density increases in the layer.

On the theoretical side, the static properties of grafted polymer layers have been extensively studied. One usually distinguishes two regimes according to the grafting density. In the mushroom regime, which is a dilute regime ($\sigma < R_G^{-2}$ where R_G is the bulk radius of gyration of the polymer chains), neighboring grafted chains do not overlap. The polymers are isolated and the only constraint is that they cannot penetrate the surface. In the brush regime ($\sigma > R_G^{-2}$), the polymers overlap and stretch in the direction normal to the surface to avoid each other. The equilibrium structure of the brush (height, chemical potential) has been extensively discussed for several years.[5,6] More recently, there has been increasing interest in the dynamical properties of grafted polymer layers. The formation of a grafted layer from a solution of end-functionalized polymers has been investigated by several groups, by experimental,[7,8] by theory,[9,10] or via computer simulations.[11] The main result is that the adsorption is a slow process, because of the high energy barrier created by already grafted chains, and that the adsorption time increases exponentially with the polymer chemical potential in the brush. Recent simulations[11] have shown that the last step of the adsorption

S0024-9297(97)01665-3 CCC: $15.00
Published on Web 03/20/1998

is a local process associated with the fluctuations of the end monomer close to the surface and independent of the rest of the chain. The inverse process, the desorption of polymers from a brush, has been studied by simulations[12,13] which show that the characteristic time grows exponentially with the grafting energy.

In order to study the relaxation of the surface density or the surface pressure in a monolayer formed by a grafted polymer layer, we build a theoretical model based on these dynamical theories for polymer brushes. Our model takes into account the fact that the polymer chains can be anchored on the surface either by one end or by both ends and allows both for exchange between these two conformations and for desorption of the polymer chains. Although a simple polymer brush model is certainly very rough for end-capped PEO monolayers, this model gives a good qualitative description of the experimental results.

This paper is organized as follows: The experimental results are presented in section 2; we present both surface pressure isotherms and relaxation curves. The typical relaxation time is studied as a function of the degree of polymerization N ($100 \leq N \leq 800$), by changing the anchoring group from C_{12} to C_{16} and the grafting density σ, which is varied over a broad range by compression of the monolayer. In section 3, we present the theoretical models describing the structure of the grafted polymer layer and the dynamic desorption process. The experimental results are compared to these theoretical predictions in section 4, where the limitations of the model are also discussed. The last section presents some concluding remarks.

2. Experimental Results

2.1. Materials. The functionalized end-capped PEO samples ($H_{25}C_{12}-O-(CH_2-CH_2-O)_N-C_{12}H_{25}$) were synthesized by G. Beinert and F. Isel in the laboratory. Commercial PEO with terminal OH groups and with narrow mass distributions was purchased and then functionalized. The synthesis details can be found in ref 14 along with a discussion of the characterization. The properties of these end-capped PEO molecules were studied in the bulk in refs 3 and 15. The PEO bi-OH used in the experiments described below are the same samples used for the synthesis of the functionnalized PEO. Four different molecular masses were studied, the masses are as announced by the producers, and the polydispersity (M_w/M_n) was measured in the laboratory by size exclusion chromatography: $M_n = 6000$ g/mol (from Hoechst $M_w/M_n = 1.04$), $M_n = 10\,000$ g/mol (from Aldrich $M_w/M_n = 1.03$), $M_n = 20\,000$ g/mol (from Hoechst $M_w/M_n = 1.01$), and $M_n = 35\,000$ g/mol (from Merck $M_w/M_n = 1.01$). These masses correspond to degrees of polymerization N equal to: 135, 230, 450, and 800, respectively. In order to study the influence of the alkyl chain length, we also used a telechelic PEO of mass 35 000 g/mol substituted by $C_{16}D_{33}$ (synthesized for neutron diffusion studies in bulk).

Both types of PEO were dissolved in chloroform (Merck pro analysi) at a concentration of about 0.2 g/L. The polymers were spread onto pure water (purified by the Milli-Q system from Millipore and used without any additive) using a microsyringe in a Langmuir trough (Lauda FW1). After 5 min, the film was compressed at constant speed and the surface pressure Π was recorded against the total area S accessible for the film. The surface pressure is directly measured in this trough as the difference between the surface tensions of pure water and of water carrying the film: $\Pi = \gamma_0 - \gamma$. To obtain the full isotherm, several depositions with different initial densities were needed. All the experiments were performed at a constant temperature 22 °C regulated by water circulation. The isotherms were recorded at a constant velocity: $v \simeq 0.5$ Å^2/monomer/min. In some experiments, the velocity was changed to study its influence on the stability of the monolayer.

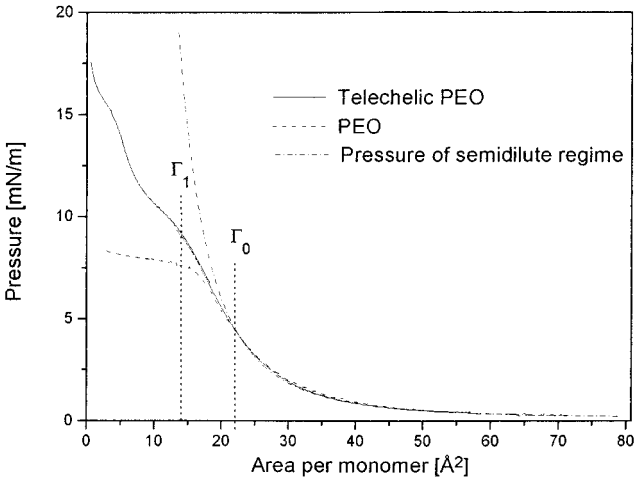

Figure 1. Surface pressure−area isotherms of PEO and telechelic PEO with $C_{12}H_{25}$ terminal groups, $N = 135$. The third curve is the pressure of the semidilute regime predicted by des Cloizeaux.

2.2. Pressure−Area Isotherms. In order to probe the influence of the hydrophobic ends on the interfacial properties of the PEO, we have compared the pressure−area isotherms of pure PEO and of telechelic PEO.

2.2.1. PEO Isotherms. PEO is known to be surface active enough to form monolayers at the air−water interface,[16,17] despite the fact that it is water soluble at room temperature.

A typical isotherm such as the one shown in Figure 1 shows three different regimes: At low density $\Gamma < \Gamma_0 = 0.3$ mg/m^2, corresponding to an area per monomer >22 Å^2, there is a semidilute regime, already described by de Cloizeaux,[18] where the surface pressure is independent of the chain length and increases as a power law of the surface density. In a good solvent the predicted scaling law is

$$\Pi = \alpha\Gamma^3 \qquad (1)$$

In our experiments, the pressure Π is expressed in mN/m, the density of monomers Γ in Å^{-2} and we find $\alpha = 46\,500$ in these units. Note that at even lower density, a dilute (ideal gas) regime exists, but it was never observed in our experiments. At higher densities, there is an intermediate regime ($\Gamma_0 < \Gamma < 0.7$ mg/m$^2 = \Gamma_1$), where the pressure continues to increase but more slowly than in the semidilute regime. Finally, in the dense range ($\Gamma > \Gamma_1$), which is the range of interest for this work, the pressure remains constant. This plateau has been interpreted[19,20] by the dissolution of PEO molecules in water. At high surface concentration, the monolayer is no longer stable and the polymer molecules are expelled from the surface, the density and therefore the pressure remaining constant. Successive compression−expansion cycles were performed and the corresponding isotherms did not coincide. In fact, they could be superimposed by a dilatation along the density axis.

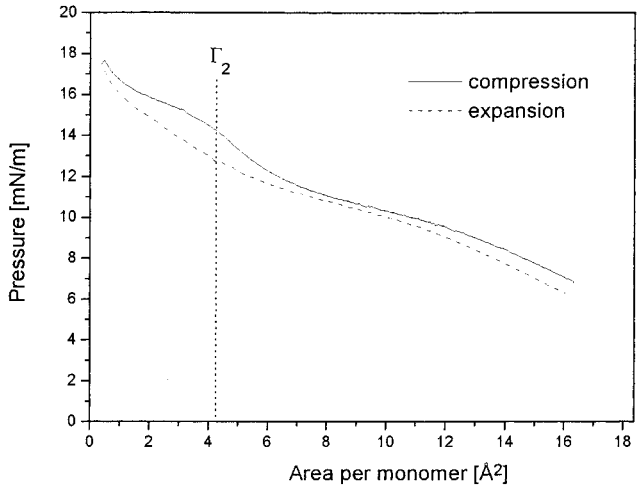

Figure 2. Surface pressure−area isotherm of telechelic PEO ($N = 135$) at high density. The hydrophobic ends are $C_{12}H_{25}$.

We interpret this misfit as a direct consequence of the loss of polymers in the bulk. During the expansion, the polymer molecules expelled in water do not come back to the surface, where the chemical potential is much higher than in the bulk ($\mu_{bulk} \ll \mu_{surface}$).

2.2.2. Telechelic PEO Isotherms. A comparison between the isotherms obtained with PEO and telechelic PEO is given in Figure 1 for the same PEO molecular mass ($M = 6 \times 10^3$ g/mol) and with $C_{12}H_{25}$ telechelic groups. At low surface coverage, before the plateau ($\Gamma < \Gamma_1$), there is no influence of the hydrophobic ends, and the isotherms are essentially identical. In the dense regime ($\Gamma > \Gamma_1$), the surface pressure of the telechelic PEO increases strongly; this is due to the anchoring of the PEO molecules on the monolayers by the hydrophobic ends. At this surface coverage, the non-end-capped PEO molecules dissolve in water. It is thus reasonable to suppose that the ethylene oxide monomers of the functionalized PEO dive into the water, while the hydrophobic ends remain at the surface. The monolayer forms therefore a grafted polymer layer under compression. This additional increase of the pressure at high surface concentration has already been observed by Kim and Cao for telechelic PEO end capped by $C_{16}H_{33}$,[4,21] but their interpretation of the phenomenon is completely different. In the following, we focus on this part of the isotherms, which we call the brush part.

Figure 2 shows in more detail the brush part of the isotherm, which can be separated into three qualitative regions: the first region corresponds to the formation and the compression of the brush, then a second plateau ($\Gamma = \Gamma_2$) appears that we interpret by the dissolution of the grafted polymers, and finally, at the highest density, the pressure diverges, due to a dynamical effect (the rate of compression is so high that the polymers have not enough time to leave the brush). For $\Gamma > \Gamma_2$, the grafted polymer layer is no longer stable, and if the compression is stopped, a relaxation of the pressure is observed corresponding to a loss of polymers in the water subphase. We also observed that successive isotherms coincide only if we stop the compression before the second plateau, which confirms the fact that the dissolution appears at densities higher than Γ_2. During the expansion of the layer, the isotherm does not present any plateau, as shown in Figure 2.

Figure 3 shows the isotherms of telechelic PEO for four different molecular masses. The surface pressure

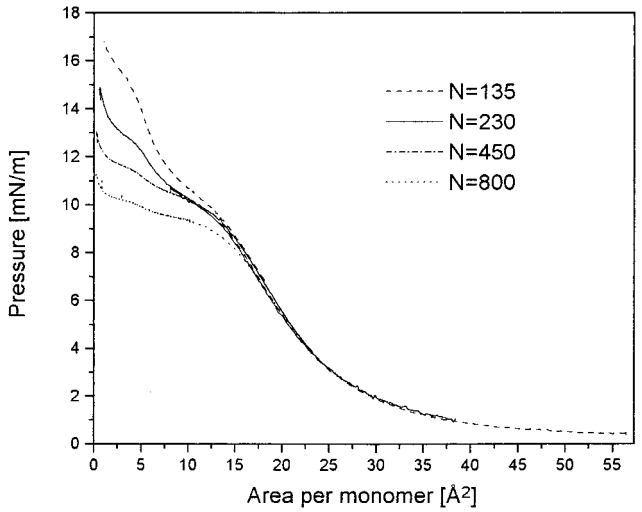

Figure 3. Surface pressure−area isotherms of telechelic PEO of different chain lengths. The hydrophobic ends are $C_{12}H_{25}$.

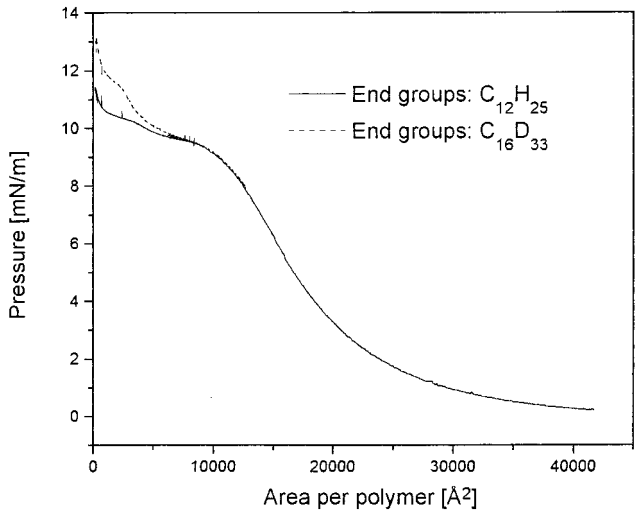

Figure 4. Surface pressure−area isotherms of two telechelic PEOs of the same number of monomers ($N = 800$) but with different end groups.

of the brush is expected to depend on the chain length N. Indeed, the isotherms, which are plotted versus the area per monomer, do not coincide, except in the semidilute regime. In the brush part, the surface pressure and the slope of the isotherms increase with decreasing N. The value of the pressure at the second plateau also increases with decreasing N. All those observations are consistent with the fact that longer polymers are more soluble and they become soluble at a smaller pressure.

Figure 4 shows the pressure−area isotherm of two different functionalized PEO ($C_{12}H_{25}$,$C_{16}D_{33}$) of the same molecular mass ($M = 35\,000$ g/mol equivalent to $N = 800$). The pressure of the plateau increases with the grafting energy, since polymers with longer hydrophobic ends are harder to dissolve.

In order to study the dynamical effects, we have varied the compression velocity. At higher velocity, the surface pressure at the second plateau increases, as shown in Figure 5. This is in agreement with the idea that this plateau corresponds to the dissolution of the molecules; if the layer is compressed faster, the density increases more, because the polymers have less time to desorb.

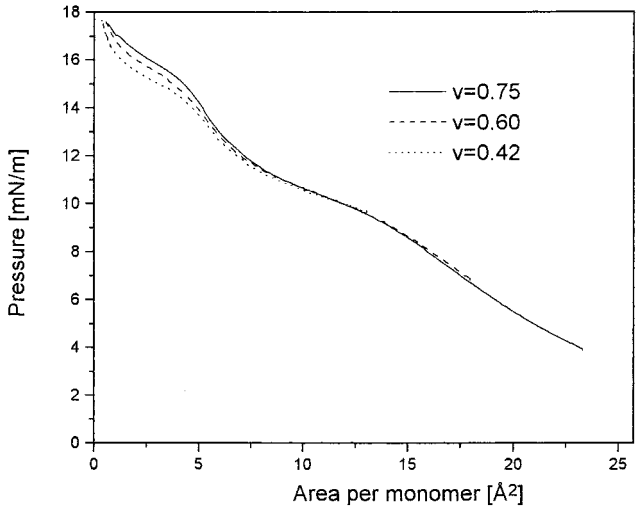

Figure 5. Surface pressure−area isotherms of telechelic PEO ($N = 135$) performed at three different compression speeds. The velocities are expressed in Å²/monomer/min.

2.3. Relaxation Kinetics. The surface pressure relaxation experiments were realized as follows. We first compressed the layer as in the isotherm measurements. We stopped the compression at different densities and measured the surface pressure relaxation over about 12 h. The main observation is that the layer is stable before the second plateau ($\Gamma < \Gamma_2$), as expected, but becomes unstable at higher surface coverage. When the compression is stopped at large densities ($\Gamma > \Gamma_2$), the pressure decreases with time and tends to a limit that does not depend on the starting point, where the compression was stopped.

The relaxation kinetics are slower with longer chains than with shorter ones: the relaxation curve of the telechelic PEO ($M = 20\,000$ g/mol) reaches a plateau after about 12 h, whereas the limit is reached after 3 h for the molecular mass ($M = 6000$ g/mol). Finally, the relaxation kinetics are slowed down when the number of carbons of the end group (or equivalently the grafting energy) increases.

3. Polymer Brush Theory

PEO shows a complex behavior in water. Bekiranov[22] has shown that a model based on the fact that the quality of the solvent changes with the concentration of the polymer reproduces well the experimental results. PEO is in a good solvent at low concentration, but the quality of the solvent decreases with increasing concentration. We study here the two extreme cases where PEO is considered as a polymer in a good solvent (with a swelling exponent $\nu = {}^3/_5$) and a θ solvent ($\nu = {}^1/_2$). We describe the structure of the grafted polymer layer by a self-consistent mean field theory in a θ solvent and by scaling laws in a good solvent.

3.1. Static Theory. In the monolayer, there is an equilibrium between three states of the PEO molecules: the bigrafted molecules are grafted to the air−water interface by their two end points, and their number is P_B; the monografted molecules are grafted only by one end point, and their number is P_M; finally, P_F molecules are not grafted to the interface and are free in the bulk water. In the following, we characterize the free polymers by their chemical potential μ_{bulk}.

All the properties of the grafted polymer layers depend on four parameters: the grafting energy Ek_BT, which is the energy cost to dissolve one hydrophobic end in water (we use here the thermal excitation k_BT as the energy unit), the chain length N, the grafting density σ (the number of grafted chains per unit area), and the composition of the layer $x = P_B/(P_B + P_M)$, which gives the fraction of bigrafted polymers. We now calculate the free energy and the surface pressure of the monolayers in the mushroom regime, when the grafted chains do not overlap, and in the brush regime.

3.1.1. Mushroom Regime ($\sigma < R_G^{-2}$). We first consider grafted polymer chains in a θ solvent. In the mushroom regime, the polymers are isolated and independent, so that the partition function of the total system is

$$Z = \frac{1}{P!}(Q)^P \tag{2}$$

where P is the total number of grafted polymers and Q is the individual partition function. In a θ solvent, there is no interaction between the monomers and the individual partition function is only the sum on all the configurations of the chain, taking into account the elastic energy of each conformation and the fact that the polymers cannot penetrate the surface; the partition function reads

$$Q = \int_{z>0} \mathrm{D}z(.)\, \exp\left[-\frac{3}{2a^2}\int_0^N \mathrm{d}s \left(\frac{\partial z}{\partial s}\right)^2\right] \tag{3}$$

where $z(s)$ is the position of the s monomer, $z(.)$ is one configuration of the chain, and $(3k_BT/2a^2)\int_0^N \mathrm{d}s(\partial z/\partial s)^2$ is the elastic energy associated with this configuration. The partition function Q is calculated exactly in Appendix 1. For one bigrafted polymer, the free energy is

$$F_B/k_BT = \frac{3}{2}\ln N - \frac{1}{2}\ln\frac{54}{\pi} \tag{4}$$

For one monografted chain

$$F_M/k_BT = \frac{1}{2}\ln N + \frac{1}{2}\ln\frac{\pi}{6} + E \tag{5}$$

The energy of configuration is smaller, because one end is free, but it costs energy to dissolve the hydrophobic end in the bulk.

The total free energy per unit area of the system is

$$F_S(N,E,x,\sigma) = x\sigma F_B + (1-x)\,\sigma F_M + xk_BT\sigma \ln x\sigma + (1-x)k_BT\sigma \ln[(1-x)\sigma] \tag{6}$$

The last two terms correspond to the entropy of mixing. The equilibrium value of the composition x_{eq} for a given value σ of the grafting density is obtained by minimization of the total free energy with respect to x:

$$x_{eq} = \frac{\alpha}{1+\alpha} \quad \text{where} \quad \alpha = \frac{3}{2N}\exp E \tag{7}$$

There is a competition between the chain length and the grafting energy. A large grafting energy increases the proportion of bigrafted polymers and a large chain length reduces it. In our experiments, typically $E = 12$, $N = 800$ (the longest chains), and $x_{eq} = 0.996$. The composition x is close to 1, and the monolayer is mostly composed of bigrafted polymers.

The surface pressure can be calculated from the free energy. In the mushroom regime, it is given by the ideal gas law ($\pi = k_B T\sigma$) and the chemical potential is $\mu = k_B T \ln \sigma$. The equilibrium with the bulk ($\mu_{bulk} = \mu_{surface}$) gives a relation between the grafting density and the bulk concentration if thermal equilibrium is reached.

In a good solvent the monomers repell each other, so that each chain is more streched than in a θ solvent. The free energy is estimated using scaling arguments. It has the same structure as in the θ solvent case but the coefficients of the logarithms are different. Duplantier[23] has defined and calculated the two surface exponents such that $F_B/k_B T \simeq \gamma_{II} \ln V$ and $F_M/k_B T \simeq \gamma_I \ln N$. The monolayer composition at equilibrium is $x_{eq} = (\exp E)/N^{\gamma_{II}-\gamma_I}$, which always remains close to 1.

3.1.2. Brush Regime ($\sigma > R_G^{-2}$). In a θ solvent, the chain radius of gyration is $R_G \propto N^{1/2}$ and the condition for overlap of the chains grafted on a surface is $R_G^2\sigma > 1$. In order to describe the thermodynamic properties of the brush, we use the self-consistent field theory first introduced by Milner, Witten, and Cates.[6] This mean field theory is based on two assumptions. First, the fluctuations around the most probable configuration of each chain are neglected, which is a good approximation in the limit of highly stretched polymers, and second, each monomer feels a mean field potential proportional to the square of the local concentration $c(z)$ (due to the third virial interaction in a θ solvent) $V(z) = wc(z)^2$. This last assumption is valid in a θ solvent, where the mean field theory is presumably exact.

The monolayer is composed of two kinds of polymers, bigrafted and monografted polymers. We use the theory of polydisperse polymer brushes,[24] by considering that a bigrafted polymer can be replaced by two monografted polymers of half-length. This assumption is supported by the fact that in the strong stretching limit, the mechanical tension vanishes at the midpoint of a bigrafted chain. With this condition, the two parts of the chain are independent of each other and can be treated as different chains of half-length. The effective grafted polymer layer that we study is composed of $2xP$ polymers of chain length $N/2$ and $(1 - x)P$ polymers of chain length N. A calculation similar to that performed by Milner et al. for polymers in a good solvent[24] gives the free energy per unit area (the only difference is that in a θ solvent, the binary repulsion is replaced by a ternary repulsion described by the mean field potential $V(z)$):

$$\tilde{F}(N,E,\tilde{\sigma},x) = \frac{1}{4}N\tilde{\sigma}^2((1+x)^2 + (1-x)^2) + (1-x)\tilde{\sigma}E + x\tilde{\sigma}\ln x\tilde{\sigma} + (1-x)\,\tilde{\sigma}\ln(1-x)\tilde{\sigma} \quad (8)$$

where $\tilde{\sigma} = \sigma\sqrt{6w/a^2}$ and $\tilde{F} = (F/k_B T)\sqrt{6w/a^2}$ are the dimensionless grafting density and the dimensionless free energy.

The first term in the expression of $\tilde{F}$ corresponds to the energy of the brush, the second corresponds to the energy of the dissolved ends, and the last two terms correspond to the mixing entropy. In the limit where the brush becomes dilute at the crossover to the mushroom regime ($N\tilde{\sigma} \to 1$), the expression of the free energy differs from that found in the mushroom regime by the logarithmic factors that are ignored in the strong stretching approximation. This remains a good approximation in the limit of stretched polymers, as long as $\ln N$ is small compared to $N\tilde{\sigma}$. The equilibrium composition of the layer x_{eq} is obtained by minimization of the free energy and satisfies the following equation:

$$N\tilde{\sigma}x_{eq} - E + \ln\frac{x_{eq}}{1-x_{eq}} = 0 \quad (9)$$

In the limit where most polymers are bigrafted $x \simeq 1$, which corresponds to our experiments, the composition can be approximated by

$$x_{eq}(N,E,\tilde{\sigma}) = \frac{\beta}{1+\beta} \quad \text{where} \quad \beta = \exp(E - N\tilde{\sigma}) \quad (10)$$

which shows the competition between the desorption energy of one end and the stretching energy to insert one chain into the brush. The chemical potential of one chain in the monolayer is

$$\frac{\mu_{brush}}{k_B T} = \frac{1}{2}N\tilde{\sigma}((1+x_{eq})^2 + (1-x_{eq})^2) + \ln\tilde{\sigma} \quad (11)$$

The condition on the density $\sigma > R_G^{-2}$ is equivalent to $\mu_{brush}/k_B T > 1$. The surface pressure is given by $\pi = \sigma(\partial F/\partial\sigma) - F$ and is proportional to $N\tilde{\sigma}^2$.

In a good solvent $R_G \propto N^{3/5}$ and the strong stretching condition for the formation of a polymer brush is $N^{6/5}\tilde{\sigma} > 1$. The structure of the brush is easily described in terms of scaling laws. The essential argument for a monodisperse polymer brush is that the chemical potential is a function of the reduced grafting density $R_G^2\sigma$ and is proportional to the number of monomers N. In order to satisfy these conditions, we impose a power law behavior $\mu \propto (R_G^2\sigma)^\delta$ and find $\mu \propto N\tilde{\sigma}^{5/6}$. By integration, we obtain the free energy per unit area and surface pressure, both proportional to $N\tilde{\sigma}^{11/6}$. For a polydisperse brush containing both monografted and bigrafted chains, the scaling laws remain identical but the prefactors vary smoothly with the composition from a finite value at $x = 0$, which corresponds to a monolayer of monografted chains, to a larger value at $x = 1$, which corresponds to a monolayer of bigrafted chains. At equilibrium, the layer is also composed mostly of bigrafted chains and the composition x is close to 1; it is given by an expression similar to (10) where the brush chemical potential $N\tilde{\sigma}$ is replaced by its value in a good solvent, $cN\tilde{\sigma}^{5/6}$ (the constant c cannot be obtained from the scaling argument).

3.2. Polymer Desorption Kinetics. At high density ($\Gamma > \Gamma_2$), we observe experimentally that the monolayer is no longer stable and that the surface pressure relaxes with time. This relaxation is related to a decrease of the density due to the desorption and the expulsion of the polymers from the brush. We thus want to describe here the nonequilibrium state of a grafted polymer layer exposed to a pure solvent. Under these conditions, the bulk concentration is extremely low and the chemical potential in the bulk is much smaller than the chemical potential in the monolayer: $\mu_{bulk} \ll \mu_{brush}$. The true equilibrium state is reached when all the polymers have desorbed from the monolayer into the bulk; however, there is a tremendous slowing down of the dynamics at long times and, in practice, the pressure relaxes only to a finite value over reasonable time scales.

3.2.1. Kinetic Equations. We describe theoretically the relaxation of the number of grafted chains by considering three dynamic processes: the desorption of

one end of a bigrafted polymer to form a monografted polymer with a characteristic time T_1, the inverse process, the adsorption of the free end of a monografted chain with a characteristic time T_2, and the desorption of a monografted polymer expelled from the brush to the bulk in a time T_3. In this model, we neglect the adsorption of the free polymer chains to the surface because of the extremely low bulk concentration or, equivalently, of the very low value of the chemical potential of the free chains.

The balance of the fluxes of incoming and outgoing chains within these approximations leads to the following kinetic equations:

$$\frac{dP_B}{dt} = -\frac{P_B}{T_1} + \frac{P_M}{T_2} \tag{12}$$

$$\frac{dP_M}{dt} = \frac{P_B}{T_1} - \frac{P_M}{T_2} - \frac{P_M}{T_3} \tag{13}$$

In the following, it is more convenient to write the kinetic equations in terms of the composition x and the grafting density $\tilde{\sigma}$:

$$\frac{d\tilde{\sigma}}{dt} = -\frac{(1-x)\tilde{\sigma}}{T_3} \tag{14}$$

$$\frac{dx}{dt} = -\frac{x}{T_1} + \frac{(1-x)}{T_2} + \frac{x(1-x)}{T_3} \tag{15}$$

The three relaxation times depend on the instantaneous thermodynamic state of the monolayer and thus on the instantaneous values of x and $\tilde{\sigma}$ (and also on the chain length N and the grafting energy E). We now build a microscopic theory to determine these relaxation times. We first calculate the two desorption times T_1 and T_3 and then estimate the adsorption time T_2 using a local equilibrium approximation. Another estimation of the adsorption time based on the decoupling of the dynamic modes of the chain, which leads to slightly different results, is given in Appendix 2.

3.2.2. Desorption Times. The desorption process occurs in two stages: the desorption of the chain hydrophobic head and the expulsion of the chain from the brush.

Wittmer and co-workers[12] have shown that the desorption of the head is a local process due to the chain-stretching fluctuations in the vicinity of the grafting surface; the relaxation time does not depend on molecular weight and depends only on the local monomer density and the grafting energy. The desorption time is

$$T_d = \tau(d_b/a)^3 \exp E \tag{16}$$

where τ is a microscopic molecular time and d_b is the size of the first concentration blob or the concentration correlation length in the vicinity of the grafting surface. The Boltzmann factor $\exp E$ is associated with the diffusion through the barrier of energy E, and $\tau(d_b/a)^3$ is the so-called Zimm time of a blob, the time to reach the "second blob", where the probability that the chain hydrophobic end point comes back to the grafting surface becomes negligible. The Zimm time takes into account the monomer−solvent friction and the hydrodynamic interactions between monomers. The size of the first blob depends on the grafting density; both in a good and a θ solvent, it can be written as

$$d_b = a\tilde{\sigma}^{-1/2} \qquad \text{in the brush regime} \tag{17}$$

$$d_b = R_G \qquad \text{in the mushroom regime} \tag{18}$$

For a brush of 5 blobs formed by polymers of $N = 800$, $E = 12$, and $\tau = 10^{-10}$ s, we find $T_d = 1.6 \times 10^{-2}$ s. Note that the precise numerical prefactor of the desorption time depends on the precise definition of the blob size and thus on the tension of the chain at the surface. The tension is slightly different for the bigrafted and the monografted chains, and thus the prefactor of the desorption time is also slightly different; we ignore this subtlety in the following.

Wittmer et al. have shown[12] that, in a grafted polymer layer, a single chain cut from the surface is driven out of the layer by the chemical potential gradient at constant velocity. This velocity is inversely proportional to the chain length N so that the expulsion time, given by $T_e = (h/2)/v$, is proportional to N^2. More precisely,

$$T_e = \tau\sigma^{1/2\nu-1} N^2 \tag{19}$$

In a θ solvent, $\nu = 1/2$ and with a polymer of chain length $N = 800$, we find $T_e = 3 \times 10^{-5}$ s. The expulsion is instantaneous compared to the desorption of the head ($T_e \ll T_d$) and can thus be ignored, so that, to a good approximation: $T_1 \simeq T_3 \simeq T_d$.

3.2.3. Adsorption Time. In order to calculate the adsorption time T_2, we assume that the monolayer is always at a local equilibrium and that the adsorption time only depends on the grafting density $\tilde{\sigma}$ and on the composition of the layer x (and not explicitly on the grafting energy E for a given composition and grafting density). At a given value of $\tilde{\sigma}$ and x, there is one value of the grafting energy E_x given by eq 9 such that the layer is at equilibrium, i.e., such that $x = x_{eq}(\tilde{\sigma},E_x)$. For this value of the grafting energy, if we ignore the chain desorption (constant σ) the inward and outward fluxes of bigrafted chains exactly compensate in eqs 13 and 15:

$$T_2 = \frac{1-x(t)}{x(t)} T_1 \tag{20}$$

The desorption time T_1 is here calculated with a grafting energy E_x related to x via eq 9. As in our experiment, x is always close to 1, we conclude that the adsorption time is small compared to the desorption time ($T_2 \ll T_1$).

In a θ solvent, in the mushroom regime, we obtain $T_2(N,E) = \tau N^{5/2}$ and in the brush regime, $T_2(N,E,\tilde{\sigma}) = \tau\tilde{\sigma}^{-3/2} \exp(xN\tilde{\sigma})$.

The adsorption time is proportional to $\exp(xN\tilde{\sigma}) = \exp(\mu_{brush})$, as the incoming chain must overcome the energy barrier created by the already grafted polymers to reach the surface and to adsorb.

We have already mentioned that, in the experimental situations we want to investigate, x is always close to 1. It is easy to check from eqs 15 and 14 and that as $T_2 \ll T_1$, x is a fast variable and σ is a slow variable. At each time, the composition relaxes to its equilibrium value at the grafting density $\tilde{\sigma}$ and it is a good approximation to replace x by its equilibrium value $x(t) \simeq x_{eq}(\tilde{\sigma}(t),E,N)$.

3.2.4. Density Relaxation. The decrease of the grafting density with time due to the desorption of the grafted chains from the monolayer follows the kinetic equation

$$\frac{d\tilde{\sigma}(t)}{dt} = -\frac{1 - x_{eq}(\tilde{\sigma}(t),N,E)}{T_3(N,E,\tilde{\sigma}(t))}\tilde{\sigma}(t) \tag{21}$$

The density of grafted polymers relaxes thus over a characteristic time T_R,

$$T_R = \frac{T_3(N,E,\tilde{\sigma})}{1 - x_{eq}(N,E,\tilde{\sigma})} \tag{22}$$

In the case where $x \sim 1$, the density relaxation time is much larger than T_3, which is the characteristic time to desorb one end from the surface. Replacing T_3 and x by their expressions (10) and (16), we find, in a θ solvent, in the mushroom regime

$$T_R = \tau N^{5/2} \exp(2E) \tag{23}$$

The relaxation time is proportional to $\exp(2E)$, since a chain has to overcome an energy barrier $2E$ to detach its two ends and to leave the surface.

In the brush regime

$$T_R = \tau\tilde{\sigma}^{-3/2} \exp(2E - N\tilde{\sigma}) \tag{24}$$

This expression shows the competition between the energy to detach the two ends and the elastic chemical potential of the chain. A large energy E increases the relaxation time and a dense brush expells polymers more easily.

A similar expression for the relaxation time of the density of grafted chains is found for a polymer layer in a good solvent using scaling laws; in the brush regime, the relaxation time is $T_R = \tau\tilde{\sigma}^{-3/2} \exp(2E - cN\tilde{\sigma}^{5/6})$. In the limit $N\tilde{\sigma} \to 1$ (or in the case of a good solvent, $N\tilde{\sigma}^{5/6} \to 1$), the preexponential factors of the relaxation times in the mushroom and the brush regimes do not crossover smoothly; this is due to the logarithmic prefactors (8) that have been ignored in the free energy in the strong stretching approximation used to describe the polymer brush.

The decrease with time of the grafting density is obtained by direct integration of eq 21:

$$t = \tau N^{3/2} \exp(2E) \int_{N\tilde{\sigma}(t)}^{N\tilde{\sigma}(0)} \frac{du}{u^{5/2} \exp u} \tag{25}$$

In this expression, the integral has a generic form, depending only on the value of the chemical potential at the beginning of the relaxation. A rescaled time appears:

$$t^*(E,N) = \frac{t}{\tau N^{3/2} \exp(2E)} = f(N\tilde{\sigma}) \tag{26}$$

Note that this time can be very large, as it increases as $\exp(2E)$; at long times, the grafting density only decreases as a power law and the relaxation is extremely slow. The same kind of calculation can be performed for a monolayer in a good solvent and we find

$$t^{**} = \frac{t}{\tau N^{9/5} \exp(2E)} = \int_{\mu(t)}^{\mu(0)} \alpha^{9/5} \frac{du}{u^{14/5} \exp u} \tag{27}$$

where μ is the chemical potential of one chain in the brush.

4. Interpretation of the Experimental Results

4.1. Isotherms. We give here a quantative interpretation of the experimental isotherms in the range $0 < \Gamma < \Gamma_2$. We know that, for $\Gamma < \Gamma_0$, all the monomers are adsorbed at the interface and form a semidilute solution in two dimensions and that, for $\Gamma > \Gamma_1$, the monolayer forms a brush. We calculate here the surface pressure in these two regimes, but not in the crossover region ($\Gamma_0 < \Gamma < \Gamma_1$) where a more detailed description of the adsorption of the monomers would be needed.

In the semidilute regime ($\Gamma < \Gamma_0$), the surface pressure is given by

$$\pi_a = \alpha(\Gamma_a)^3 \tag{28}$$

where Γ_a is the monomer density. The chemical potential of one chain is

$$\mu_a = \frac{3}{2}\alpha N(\Gamma_a)^2 - eN \tag{29}$$

with N the number of monomers and e the adsorption energy per monomer. In this density range, all the monomers are adsorbed and $\Gamma_a = \Gamma = 1/A$, where A is the area per monomer.

In the other regime ($\Gamma > \Gamma_1$), we will assume that there is an equilibrium between only two kinds of polymers: some of the polymers are totally adsorbed on the surface, and the other polymers are grafted to the surface by their ends but their monomers are dangling in water. This model is rather extreme and neglects the intermediate case of polymers forming many loops on the surface. We also suppose that the two types of chains are ideally mixed and that the pressure is the sum of the partial pressures:

$$\pi_{the}(\Gamma) = \pi_a(\Gamma_a) + \pi_b(\Gamma_b) \tag{30}$$

where

$$\pi_b = k_B T \sqrt{\frac{6w}{a^2}} \frac{1}{N}(\Gamma_b)^2 = \beta\frac{1}{N}(\Gamma_b)^2 \tag{31}$$

π_b is the pressure created by a brush of bigrafted polymers (8) in a θ solvent, where we neglect the entropic part. By integration of (31), we obtain the chemical potential of a bigrafted chain:

$$\mu_b = 2\beta\Gamma_b \tag{32}$$

At equilibrium, the chemical potentials of the two types of polymers are equal

$$\mu_a(\Gamma_a) = \mu_b(\Gamma_b) \tag{33}$$

and the densities are such that

$$\Gamma_a + \Gamma_b = \Gamma = \frac{1}{A} \tag{34}$$

This last equation is valid as long as no desorption takes place. By solving the two equations (33) and (34), we obtain the dependence of the densities Γ_a and Γ_b as

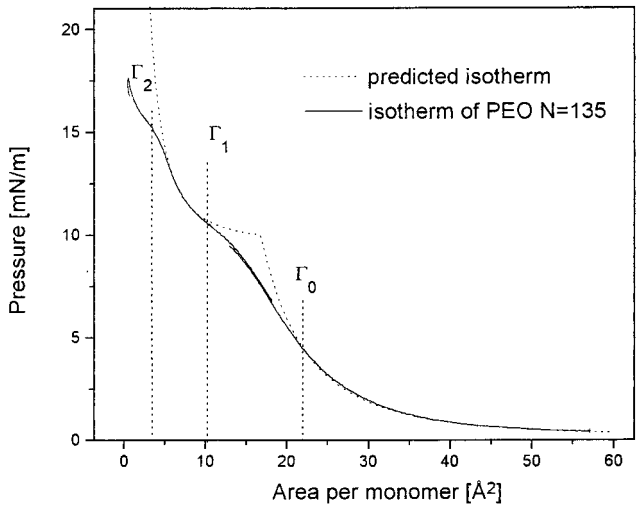

Figure 6. Comparison between the surface pressure−area isotherm of telechelic PEO ($N = 135$) and the theoretical curve π_{the}.

functions of the area per monomer A. We can then compute the pressure, $\pi_{the}(A)$, given by (30).

We can notice that μ_a is negative as long as $\Gamma < \sqrt{2e/3\alpha}$ and that μ_b is always positive. As a consequence, an equilibrium between the adsorbed polymers and the grafted polymers is possible only above $\Gamma_c = \sqrt{2e/3\alpha}$; for smaller densities, there is no polymer brush. The minimal value Γ_c increases with the adsorption energy of each monomer, which is consistent with the fact that a larger compression is needed to obtain grafted polymers, if the adsorption of the monomers is stronger. In this approach, there are two unknown parameters, the monomer adsorption energy e, and the third virial coefficient $\sqrt{6w/\alpha^2}$. To determine them, we compare the isotherm of a telechelic PEO ($N = 135$) to the theoretical curves $\pi_{th}(A)$ and we choose the parameters in the way that the two curves coincide, as shown in Figure 6.

We obtain the following values: $e = 0.6\ k_BT$ and $\sqrt{6w/\alpha^2} = 40$ Å^2. We keep these values fixed for the study of telechelic PEO of other chain lengths, because these parameters must be independent of the number of monomers N. For any chain length, the measured pressure−area isotherm and the theoretical curve coincide well in the two regimes ($\Gamma < \Gamma_0$, $\Gamma_1 < \Gamma < \Gamma_2$). The theoretical pressure does not fit the crossover, as expected, and the highest density range ($\Gamma > \Gamma_2$). In this last regime, the theoretical pressure increases faster than the real pressure, because the model considers a stable layer with a constant number of polymers at the interface and does not take the desorption of the polymers into account. However, for the longest sample ($N = 800$), we find a value of e about 4% smaller.

4.2. Desorption and Shape of the Isotherms. In this section, we focus on the brush part of the isotherm ($\Gamma > \Gamma_1$) and more precisely on the denser regime ($\Gamma > \Gamma_2$). We want to explain the presence of the second plateau in the pressure−area isotherm. During the compression of the monolayer, there is a competition between the mechanical compression that tends to increase the density and the desorption of the polymers. The evolution of the grafting density is due to the

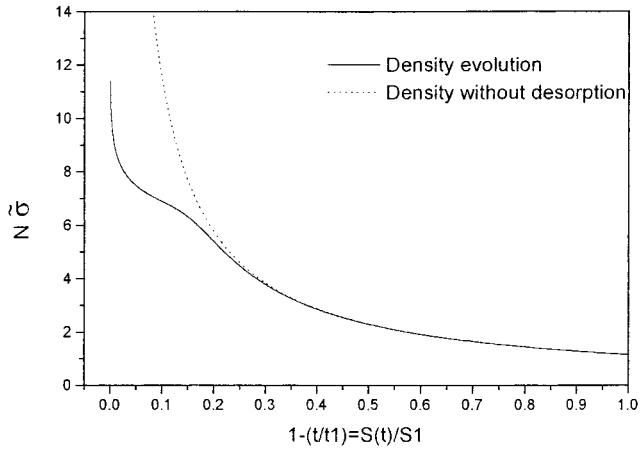

Figure 7. Theoretical evolution of the density for $N = 230$. $E = 15$ (full line) and $E = \infty$ (dashed line), i.e., without desorption.

competition between these two effects and the time derivative of the grafting density can be written as

$$\frac{d\tilde{\sigma}}{dt} = -\frac{\tilde{\sigma}}{T_R(N,\tilde{\sigma},E)} + \frac{\tilde{\sigma}}{t_1 - t} = \sqrt{\frac{6w}{a^2}}\left(\frac{1}{S}\frac{dP}{dt} - \frac{P}{S^2}\frac{dS}{dt}\right) \tag{35}$$

where P is the number of grafted polymers and $S(t)$ is the total surface at time t. We consider here the case where the barrier of length L on the trough moves at a constant velocity v; $t_1 = S_1/Lv$ is the time to compress the layer from S_1 to 0. The relaxation time T_R has been calculated in the previous section; we use the value obtained in a θ solvent, which includes all numerical prefactors. The dominant contribution in the evolution of the grafting density $\tilde{\sigma}(t)$ (35) can be identified by comparing the characteristic time scales T_R and $t_1 - t$. At the beginning of the compression, $N\tilde{\sigma} \simeq 1$, $T_R = \tau N3/2$ exp(2E - 1), and $(t_1 - t) \simeq t_1$. With $E = 15$, $N = 135$, and $\tau = 10^{-10}$ s, $T_R \simeq 170$ h, which is larger than $t_0 \simeq {}^1/_2$ h. In this limit, the second term in (35), corresponding to the mechanical compression, is dominant and the grafting density increases as observed in the experiments. But the increase of the density induces (24) a decrease of T_R, until a point where the rates of compression and desorption of the polymers are equal. This happens for

$$\tau\tilde{\sigma}_p^{-3/2} \exp(2E - N\tilde{\sigma}_p) = (t_1 - t) \tag{36}$$

The solution of this equation (36) shows that the density grows very slowly with time (logarithmically) and thus reaches a pseudoplateau.

We solved numerically eq 35 for $0 < t < t_1$ and the solution shown in Figure 7 behaves qualitatively in the same way as the measured isotherms if we plot $\tilde{\sigma}$ versus $(1 - t/t_1) = S(t)/S_1$ (note that the experimentally measured quantity is the pressure that increases monotonically with $\tilde{\sigma}$, $\pi \propto N\tilde{\sigma}^2$). The curve presents first an increase of the density, then a pseudoplateau, which corresponds to the compensation of the two processes, and finally a divergence of the density, when $(1 - t/t_1) \to 0$ (equivalent to $S(t) \to 0$). This divergence comes from the fact that the rate of compression $\tilde{\sigma}/(t_1 - 1)$ also diverges. This strongly suggests that the second plateau indeed corresponds to an important loss of polymer.

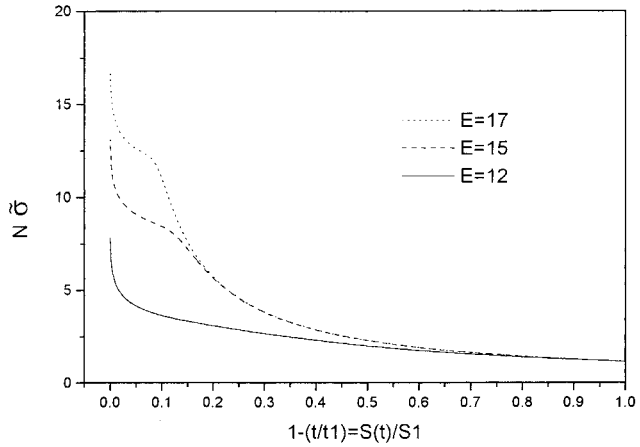

Figure 8. Theoretical variation of the density with the grafting energy.

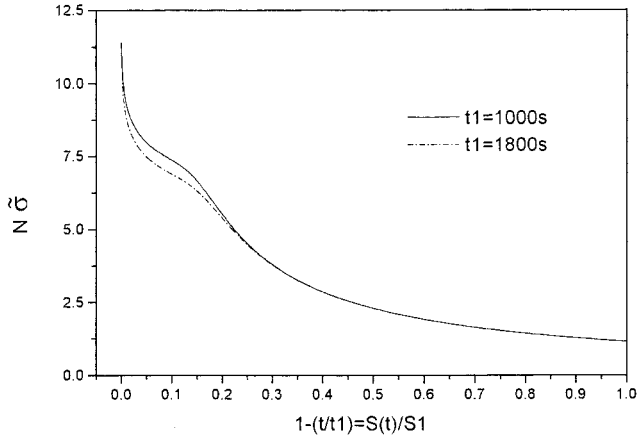

Figure 9. Theoretical variation of the density evolution with the compression velocity.

It also shows that polymers start to leave the surface before the pseudoplateau, but not in a significant way.

Equation 36 also gives a good description of the influence of the grafting energy on the shape of the curves. If E is too small and $T_R(N,\sigma(0),E) \simeq t_1$, (that corresponds in the model to $E \leq 12$), the curves $\tilde{\sigma}(t)$ present only a pseudoplateau and a divergence, because desorption already appears at the beginning of the compression. The grafting energy of one $C_{12}H_{25}$ is therefore larger than this minimal value of 12 k_BT, since we have never observed this behavior with the different telechelic PEOs that we have studied.

For two polymers of the same length, compressed at the same velocity but with different hydrophobic ends, the model predicts that the pseudoplateaus do not coincide (Figure 8). Indeed, the pseudoplateau of the polymer whose ends are more hydrophobic appears at a higher density than that of the other polymers. The reason is that the more hydrophobic ends provide a stronger anchoring to the surface, in good agreement with the experiments of Figure 4.

For the influence of the velocity (Figure 9), the model predicts that a higher compression velocity induces a pseudoplateau appearing at higher density, as observed experimentally, Figure 5.

Finally, we studied the influence of the chain length. We solved (35) for different values of the chain length (N = 135, 230, 450, 800) and calculated $\pi_{the} = \tilde{\sigma} + N\tilde{\sigma}^2$ (Figure 10). The influence of the chain length is the same as observed in the experiments, Figure 3. During

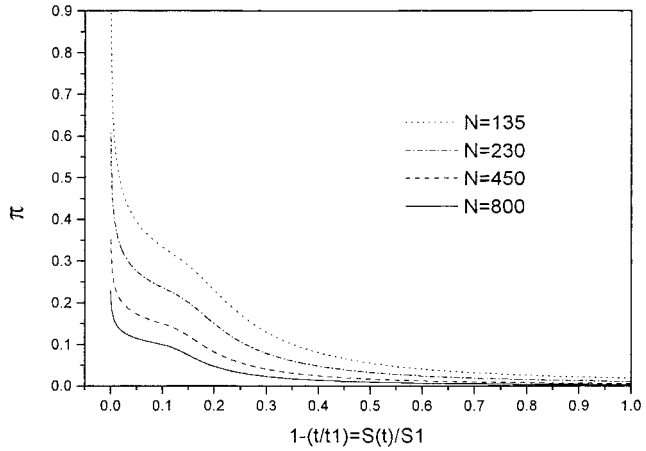

Figure 10. Theoretical model of the pressure evolution with the chain length.

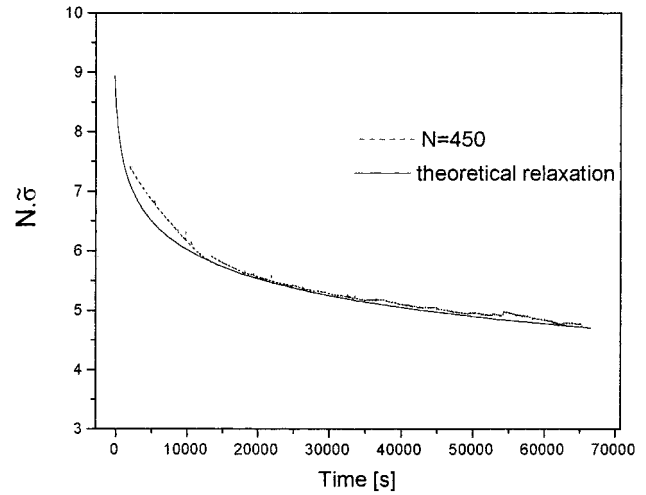

Figure 11. Comparison between the experimental relaxations of a telechelic PEO (N = 450) and the theoretical one. The value of $\tau \exp(2E)$ is 10^{-10} exp 34 s.

the expansion of the layer, the model shows no competition and no pseudoplateau, because the mechanical expansion and the desorption of the polymers both contribute to a decrease of the density:

$$\frac{d\tilde{\sigma}}{dt} = -\frac{\tilde{\sigma}}{T_R(N,\tilde{\sigma},E)} - \frac{\tilde{\sigma}}{t_1 - t} \qquad (37)$$

This is in a good agreement with the experiments; the isotherms present no plateau during the expansion, as shown in Figure 2.

4.3. Relaxation. Experimentally, we measure the pressure relaxation and the theory predicts (21) the relaxation of the grafting density $\tilde{\sigma}$. In order to make a quantitative comparison, we need to find the monomer density $\Gamma_b(t)$ corresponding to each value of the measured surface pressure $\pi_{exp}(t)$. This is done by using eq 30:

$$\pi_{exp}(t) = \pi_{the}(\Gamma) \qquad (38)$$

from where we extract $\Gamma_b(t)$. Finally, we compare the theoretical relaxation of $N\tilde{\sigma}(t)$ to the experimental relaxation, $\sqrt{6w/a^2}\Gamma_b(t) = 40\Gamma_b(t)$.

For telechelic PEO of molecular mass 20 000 g/mol (equivalent to N = 450), we see in Figure 11 that the theoretical and experimental curves coincide over 12 h.

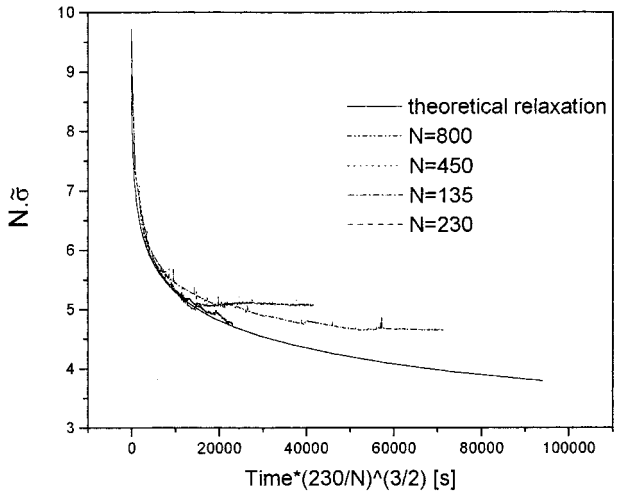

Figure 12. Experimental relaxations of telechelic PEO of all chain lengths plotted versus the rescaled time $t(230/N)^{3/2}$.

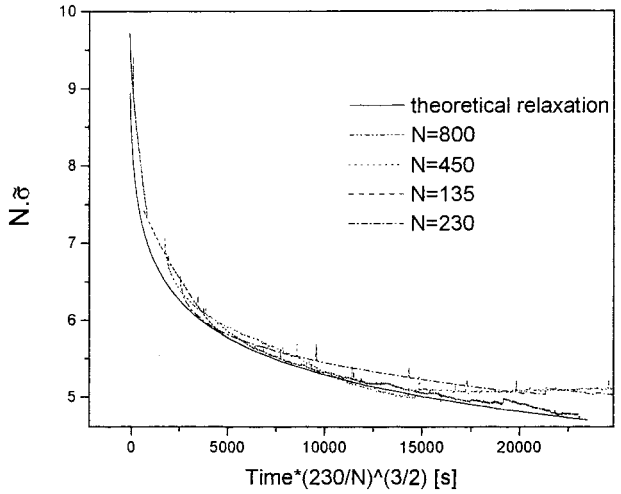

Figure 13. Zoom of Figure 12.

For the telechelic PEO of $N = 135$, we see in Figure 12 that the two curves coincide only at the beginning of the relaxation and diverge afterward. The experimental and theoretical curves do not tend to the same limit. In fact, the theory and the experiment differ when $N\tilde{\sigma} < 5.5$, where the theory of stretched polymers is no longer valid. Indeed, when the grafting density becomes too small, the monomers have more space to readsorb at the surface and the polymers form many loops. The adsorption of monomers on the surface increases the desorption time and slows down the relaxation. This is why the experimental curve, at small grafting density, relaxes slower than the theoretical one.

The comparison between the experimental relaxation and the theoretical one shows that $\tau \exp(2E) = 10^{-10}$ exp 34 s, which gives a value for E of about 17 k_BT with $\tau = 10^{-10}$ s.

We performed the same analysis for the telechelic PEO of all chain lengths ($N = 135$, 230, 450, 800) and found the same value of $\tau \exp(2E)$.

Finally, in order to test the theory and the predicted scaling laws (26), we plot $40\Gamma_b(t) = N\tilde{\sigma}(t)$, which we obtained during the relaxations of all chain lengths, versus the normalized time $t(230/N)^{3/2}$. For the telechelic PEO with $N = 230$, the rescaled time is the real time. In Figures 12 and 13, we see that all curves collapse on a single curve as long as $40\Gamma_b(t) > 5.5$. This collapse is predicted by the theory (26) and proves that the scaling laws describe well the desorption kinetics in the brush regime.

So far we have used the theoretical predictions for a polymer in a θ solvent. In the theory for a polymer in a good solvent, the dynamical study predicts (27) that the relaxation curves of polymer of different chain lengths collapse, if one plots the chemical potential proportional to $N\tilde{\sigma}^{5/6}$ versus the rescaled time $t/N^{9/5}$. This has been done for the four different chain lengths, and the different relaxation curves superimpose as well as in Figure 12. It means that the scaling laws in good solvent also describe well the relaxation and the loss of polymers. But the conclusion is that we cannot tell apart good solvent from θ solvent behavior with this kind of analysis.

We also measured the relaxation kinetics of telechelic PEO with $C_{16}D_{33}$ hydrophobic ends, the pressure relaxes slower than for telechelic PEO with $C_{12}H_{25}$ hydrophobic ends with $\tau \exp(2E) \simeq 10^{-10}$ exp 38 s corresponding to $E(C_{16}D_{33}) \simeq 19\ k_BT$. This result was, however, obtained with a single chain length ($N = 800$) and must be confirmed by other experiments on this telechelic PEO of different molecular weights.

5. Conclusion

In this work, we have studied the properties of telechelic PEO grafted at the air−water interface by hydrophobic chain ends. The comparison with monolayers of pure PEO clearly shows the importance of the hydrophobic end groups, which anchor the PEO at the surface under compression. The experiments at higher compressions show that, despite their hydrophobic ends, the polymers can detach from the interface and are then expelled from the adsorbed layer toward the bulk solution. We have studied in detail the desorption kinetics of the bigrafted polymers associated with this loss of polymers from the monolayer.

In order to interpret quantitatively these results, we have developed a static and dynamic model based on the theory of polymer brushes. The comparison between theory and the experiments shows that the static model does not reproduce the isotherms over the whole range of surface densities; it is oversimplified and ignores the adsorbed chain configurations where the chains forms trains and loops close to the surface, which turn out to be very important in the intermediate range of densities. We will try to improve our model to take this effect into account in a future work.

However, at high densities, the model describes well the desorption kinetics and gives a good description of the relaxation of the density and of the effect of the chain length, of the compression velocity, and of the grafting energy on this dynamical process. This good agreement is explained by the fact that at high density, monomer adsorption can be neglected. Finally, the comparison between the experimental and theoretical relaxation curves has allowed an estimation of the value of the grafting energy of the hydrophobic ends. The value obtained for $C_{12}H_{25}$, $E \simeq 17\ k_BT$, is higher than what is found in the literature[25] from solubility measurements, but our model does not consider an energy barrier for adsorption and desorption of the hydrophobic ends.

Acknowledgment. We are greatful to F. Isel, G. Beinert, and J. François (ICS Strasbourg, France) for

having provided the telechelic PEO used in this study. We also thank A. Johner and J. François for illuminating discussions and C. Ybert and T. Senden for helping us to solve experimental difficulties.

Appendix 1: Free Energy of a Single Grafted Polymer in a Θ Solvent

Individual Chain Partition Function. In a θ solvent, there is no interaction between the monomers, and the individual chain partition function is

$$Q = \int \mathrm{d}z(.)\, \exp\left[-\frac{3}{2a^2}\int_0^N \mathrm{d}s \left(\frac{\partial z}{\partial s}\right)^2\right] \qquad (39)$$

where $z(.)$ represents all the configurations of a given chain and where $z > 0$, because the polymer is close to an inpenetrable wall. The sum is taken over all monomers s ($s = 0$ is the monomer away from the surface and $s = N$ is the other end close to the surface). In order to compute Q, one introduces the segment probability amplitudes defined by

$$q(z,t) = \int \mathrm{d}z(.)\, \delta(z(t) - z)\, \exp\left[-\frac{3}{2Na^2}\int_0^t \mathrm{d}u \left(\frac{\partial z}{\partial u}\right)^2\right] \qquad (40)$$

and

$$q^*(z,t) = \int \mathrm{d}z(.)\, \delta(z(t) - z)\, \exp\left[-\frac{3}{2Na^2}\int_t^1 \mathrm{d}u \left(\frac{\partial z}{\partial u}\right)^2\right] \qquad (41)$$

where we have defined the reduced variable $t = s/N$.

The product $q(z,t)\, q^*(z,t)$ is the unnormalized probability to find the polymer segment t at position z. The partition function is obtained by integration of this probability. In the absence of interactions, the probability amplitudes are solutions of the free diffusion equation,

$$\frac{\partial q(z,t)}{\partial t} = \frac{Na^2}{6}\frac{\partial^2 q(z,t)}{\partial z^2} \qquad (42)$$

and

$$\frac{\partial q^*(z,t)}{\partial t} = -\frac{Na^2}{6}\frac{\partial^2 q^*(z,t)}{\partial z^2} \qquad (43)$$

The relevant solution of the diffusion equation depends on the initial condition: if the end ($t = 0$) of a polymer is localized at $z = z_0$, $q(z,t{=}0) = \delta(z - z_0)$, the solution of (42) can be derived using the method of images. It is given by

$$q(z,t) = \sqrt{\frac{3}{2Na^2t\pi}}\left[\exp\left(-\frac{3(z - z_0)^2}{2Na^2t}\right) - \exp\left(-\frac{3(z + z_0)^2}{2Na^2t}\right)\right] \qquad (44)$$

The solution for $q^*(z,t)$ can be calculated in a similar way by replacing t by $1 - t$.

Free Energy of a Polymer Grafted by One End. For a polymer grafted by one end on the surface, the end $t = 1$ is close to the surface (within a distance d, $q^*(z,t{=}1) = d\delta(z - d)$ and the other end $t = 0$ is free $q(z,t{=}0) = 1$). The length d is the order of magnitude of the monomer size a. The partition function is

$$Q_\mathrm{M} = \int_0^\infty \mathrm{d}z\, q^*(z,t{=}0) = \int_0^\infty \mathrm{d}z \sqrt{\frac{3}{2Na^2\pi}}\left[\exp\left(-\frac{3(z - d)^2}{2Na^2}\right) - \exp\left(-\frac{3(z + d)^2}{2Na^2}\right)\right] \qquad (45)$$

which can be reduced to

$$Q_\mathrm{M} = d\int_{-d}^{d} \mathrm{d}u \sqrt{\frac{3}{2Na^2\pi}} \exp\left(-\frac{3u^2}{2Na^2}\right) \qquad (46)$$

At first order in d,

$$Q_\mathrm{M} = 2d^2\sqrt{\frac{3}{2Na^2\pi}} = \frac{d^2}{a}\sqrt{\frac{6}{N\pi}} \qquad (47)$$

and the free energy is

$$\frac{F_\mathrm{M}}{k_\mathrm{B}T} = -\ln Q_\mathrm{M} = \frac{1}{2}\ln N + cst \qquad (48)$$

Free Energy of a Polymer Grafted by Their Two Ends. If the polymer is grafted by its two ends to the surface, the two ends are close to the surface, $q(z,t{=}0) = d\delta(z - d)$ and $q^*(z,t{=}1) = d\delta(z - d)$. One calculates Q_B at $t = 0$ and

$$Q_\mathrm{B} = \int_0^\infty \mathrm{d}z\, q^*(z,t{=}0)\, q(z,t{=}0) = \mathrm{d}q^*(z{=}d,t{=}0) \qquad (49)$$

Using the expression (44) of $q^*(z,t)$, one finds

$$Q_\mathrm{B} = d^2\sqrt{\frac{3}{2Na^2\pi}}\left[1 - \exp\left(-\frac{6d^2}{Na^2}\right)\right] \qquad (50)$$

The exponential can be expanded and

$$Q_\mathrm{B} = d^2\sqrt{\frac{3}{2Na^2\pi}}\frac{6d^2}{Na^2} \qquad (51)$$

so that the free energy is

$$\frac{F_\mathrm{B}}{k_\mathrm{B}T} = \frac{3}{2}\ln N + cst \qquad (52)$$

Appendix 2: Adsorption Time T_2

Model. In this appendix, we calculate the characteristic time for the free end of a monografted polymer to diffuse through the brush and adsorb on the surface. As suggested by the experiments, we focus on a grafted layer composed mainly of bigrafted polymers ($x \simeq 1$). In this limit, the height of the brush and the mean field potential are given by

$$h = Na\sqrt{\frac{2\tilde{\sigma}}{3}}\frac{1}{\pi} \qquad (53)$$

and

$$V(z) = A - B(h - z)^2 \quad \text{where} \quad B = \frac{\pi^2}{2(Nb)^2} \qquad (54)$$

For the sake of simplicity, we study only half of the

monografted polymer outside the brush and the time it needs to come back to the surface. The central monomer of the monografted chain is fixed at the position $z(n=0,t) = 0$ and the nonadsorbed chain end is free $(\partial z/\partial n)(n = N/2, t) = 0$. This model neglects all the fluctuations of the already grafted part of the chain but this approximation becomes good in the later stage of the adsorption, when the two parts are streched and when the tension in the midpoint vanishes. The latest stages give the dominant contribution to the adsorption time since it grows exponentially with the energy barrier, which is highest close to the surface.

Rouse Equation of Motion. As a first approximation, we describe the motion of the chain by the Rouse model, which neglects the hydrodynamic interactions. The equation of motion in the mean field potential $V(z)$ is given by

$$\xi\frac{\partial z(n,t)}{\partial t} = \frac{k_B T}{b^2}\frac{\partial^2 z(n,t)}{\partial n^2} - 2B(h - z(n,t)) + f_n(t) \qquad (55)$$

The random Langevin force $f_n(t)$ satisfies

$$\langle f_n(t)\rangle = 0 \qquad \text{and} \qquad \langle f_n(t)\, f_m(t')\rangle = 2k_B T\xi\delta_{n,m}\delta(t - t') \qquad (56)$$

The left-hand side of the Rouse equation is the viscous drag on monomer n located at $z(n,t)$, which is proportional to the velocity of the monomer with a microscopic friction constant ξ. The friction force is balanced by the Gaussian elastic force, the excluded volume force, and the Langevin force. The Rouse equation is solved by decomposing $z(n,t)$ as a sum of eigenmodes. Due to the boundary conditions, only the odd modes contribute.

$$z(n,t) = \sum_{p:\text{odd}}^{\infty} a_p(t)\sin\frac{np\pi}{N} \qquad (57)$$

$$f_n(t) = \sum_{p:\text{odd}}^{\infty} f_p(t)\sin\frac{np\pi}{N} \qquad (58)$$

with

$$a_p(t) = \frac{4}{N}\int_0^{N/2} \mathrm{d}n\; z(n,t)\sin\frac{np\pi}{N} \qquad (59)$$

The equation of motion then becomes

$$\xi\frac{\partial a_p(t)}{\partial t} = -k_B T\left(\frac{\pi}{Nb}\right)^2(p^2 - 1)a_p(t) - F_p + f_p(t) \qquad (60)$$

where $F_p = 8Bh/p\pi$ is a constant force, which tends to expell the chain outside the brush, and the Langevin force $f_p(t)$ verifies

$$\langle f_p(t)\, f_q(t')\rangle = \frac{8k_B T}{N\xi}\delta_{p,q}\delta(t - t') \qquad (61)$$

The amplitudes $a_p(t)$ have the following moments:

$$\langle a_1(t) - a_1(0)\rangle = -\frac{F_1}{\xi}t \qquad (62)$$

$$\langle (a_1(t) - a_1(0))^2\rangle = \left(\frac{F_1}{\xi}t\right)^2 + \frac{8k_B T}{N\xi}t \qquad (63)$$

$$\langle a_p(t) - a_p(0)\rangle = -\frac{F_p\tau_p}{\xi}\left(1 - \exp\frac{-t}{\tau_p}\right) \qquad (64)$$

$$\langle (a_p(t) - a_p(0))^2\rangle = \left(\frac{F_p\tau_p}{\xi}\left(1 - \exp\frac{-t}{\tau_p}\right)\right)^2 + \frac{4k_B T\tau_p}{N\xi}\left(1 - \exp\frac{-2t}{\tau_p}\right) \qquad (65)$$

where $\tau_p = \xi/2B(p^2 - 1)$ is the relaxation time of the mode a_p.

Fokker−Planck Equation. For each eigenmode, a Fokker−Planck equation can be written[26] using the jump moments $(\lim_{t\to 0}(\langle a_p(t) - a_p(0)\rangle/t) = -F_p/\xi)$ and $(\lim_{t\to 0}(\langle (a_p(t) - a_p(0))^2\rangle/t = 8k_B T/N\epsilon)$:

$$\frac{\partial P(a_p,t)}{\partial t} = \frac{\partial(F_p/\xi)\, P(a_p,t)}{\partial a_p} + \frac{4k_B T}{N\xi}\frac{\partial^2 P(a_p,t)}{\partial {a_p}^2} \qquad (66)$$

The amplitude of each mode diffuses in an external potential $F_p a_p/\xi$, which is p dependent. The diffusion constant $D = (2k_B T)/((N/2)\xi)$ is independent of p and is equal to twice the translational diffusion constant of a free chain in solution, because one end of the chain is fixed. As a linear combination of the modes, the position of the chain end $z(n=N/2,t) = z(t)$ is a Gaussian variable, its average value is

$$\langle z(t) - z(0)\rangle = \langle \Delta z(t)\rangle = -\frac{F_1}{\xi}t - \sum_{\substack{p\geq 3\\ :\text{odd}}}\frac{F_p\tau_p}{\xi}\left(1 - \exp\frac{-t}{\tau_p}\right)\sin\left(\frac{p\pi}{2}\right) \qquad (67)$$

and

$$\lim_{t\to 0}\frac{\langle \Delta z(t)\rangle}{t} = -\frac{F_1}{\xi}\sum_{k=0}^{\infty}\frac{1}{2k+1} = -\frac{F_1\pi}{4\xi} \qquad (68)$$

The variance is given by

$$\langle (\Delta z(t) - \langle \Delta z(t)\rangle)^2\rangle = \frac{8k_B T}{N\xi}t + \sum_{k=1}^{\infty}\frac{4k_B T\tau_{2k+1}}{N\xi}\left(1 - \exp\frac{-2t}{\tau_{2k+1}}\right) \qquad (69)$$

One checks here that no jump moment of second order can be constructed, so that no monovariant Fokker−Planck equation can be derived. We will write here an approximate Fokker−Planck equation by taking into account only the first mode:

$$\frac{\partial P(z,t)}{\partial t} = \frac{\partial(F_1/\xi)\, P(z,t)}{\partial z} + \frac{4k_B T}{N\xi}\frac{\partial^2 P(z,t)}{\partial z^2} \qquad (70)$$

First-Passage Time. In order to calculate the adsorption time, it is necessary to calculate the probability $f_{z_0}(h,t)$ for the end, starting at the position $z =$

z_0, to reach the surface after a time t. The adsorption time is equal to the first passage time[26] of the chain end on the surface and can be calculated as

$$T_{z_0} = \frac{\int_0^\infty \mathrm{d}t\ t f_{z_0}(h,t)}{\int_0^\infty \mathrm{d}t\ f_{z_0}(h,t)} = \frac{\int_0^\infty \mathrm{d}t\ t\dfrac{\partial P}{\partial z}(z=h)}{\int_0^\infty \mathrm{d}t\ \dfrac{\partial P}{\partial z}(z=h)} \qquad (71)$$

with the boundary conditions: $P(z,t=0) = \delta(z - z_0)$. A simple way to solve this equation is to use the formalism of Laplace transforms. We define $P^*(z,s) = \int_0^\infty \mathrm{d}t\ P(z,t) \exp(-st)$. The first passage time and the Fokker–Planck equation can be written as

$$T_{z_0} = \frac{-\left(\dfrac{\partial}{\partial s}\dfrac{\partial P^*}{\partial z}\right)_{z=h,s=0}}{\left(\dfrac{\partial P^*}{\partial z}\right)_{z=h,s=0}} \qquad (72)$$

$$sP^*(s,z) - \delta(z - z_0) = \frac{\partial(F_1/\xi)P^*}{\partial z} + \frac{4k_BT}{N\xi}\frac{\partial^2 P^*}{\partial z^2} = -\frac{\partial j^*(s,z)}{\partial z} \qquad (73)$$

One has to solve this equation (73) in the two space regions (region 1 where $z < z_0$ and region 2 where $z_0 < z < h$) with the boundary conditions

$$P_1^*(s,z_0) = P_2^*(s,z_0) \quad \text{and} \quad j_2^*(s,z) - j_1^*(s,z) = 1 \qquad (74)$$

In order to calculate the first passage time, we also must impose that the surface absorbs the adsorbing chain end at $z = h$ and

$$P_2^*(s,h) = 0 \qquad (75)$$

The final expression for the first passage time is

$$T_{z_0} = \frac{1}{D}\int_{z_0}^{h} \mathrm{d}z \exp U(z) \int_{z_0}^{z} \mathrm{d}z' \exp(-U(z')) \qquad (76)$$

where $U(z) = F_1 z/D\xi = 2BNhz/\pi$ is the energy barrier. In the case $z_0 = 0$, the dominant contribution to the adsorption time is

$$T = \frac{1}{6}\frac{a^2}{D\tilde{\sigma}}\exp\left(\frac{2}{\pi}N\tilde{\sigma}\right) \qquad (77)$$

The prefactor $a^2/D\tilde{\sigma}$ is the time τ to diffuse on the first blob in the Rouse model ($\tau_{\text{Rouse}} \propto (\zeta_{\text{first blob}})^2$ with $\zeta_{\text{first blob}} = (\tilde{\sigma})^{-1/2}$). The energy barrier has the same dependence on N and $\tilde{\sigma}$ as in the expression of the adsorption time found in the text (24), but the numerical prefactor is different, as we have considered here only the first eigenmode and ignored all the others.

Hydrodynamic Interactions. In a solvent, hydrodynamic interactions must be taken into account. In a dense solution, they are screened and the velocity decays with a characteristic length ζ_{eff} depending on the local concentration of monomers. On sizes smaller than ζ_{eff}, the dynamics is Zimm-like; at larger length scales, hydrodynamic interactions do not play any role and the dynamics is Rouse-like or dominated by entanglements of a Rouse-type dynamic. In ref 27, an effective monomer friction depending on the position is introduced and it is shown that the diffusion coefficient of the whole chain is $D = k_BT/6\alpha\pi\eta h$ where α is a numerical constant of the order of 1. Moreover, the final step of the adsorption process is determined by the fluctuations of the end monomer around its average position,[11] and the important length scale is the distance to the surface ($h - z$). In order to take this effect into account, we introduce a diffusion coefficient depending on the position z:

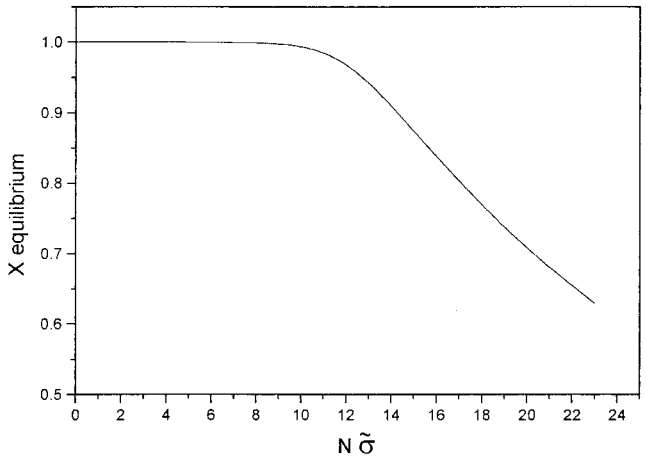

Figure 14. Proportion of bigrafted polymers at equilibrium versus $N\tilde{\sigma}$ with $E = 15$.

$$D(z) = \frac{k_BT}{6\alpha\pi\eta(h - z)} \qquad (78)$$

With this approximation for the diffusion constant, the adsorption time is calculated as

$$T = \frac{a^2}{D_0(\tilde{\sigma})^{3/2}}6^{3/2}\gamma\left(4,\sqrt{\frac{2}{\pi}N\tilde{\sigma}}\right)\exp\left(\frac{2}{\pi}N\tilde{\sigma}\right) \qquad (79)$$

where $D_0 = k_BT/6\alpha\pi\eta a$ and $\gamma(n,z)$ is the gamma function defined in ref 28 ($\gamma(n,z) = \int_0^z \mathrm{d}u\ u^{n-1} \exp u$). One finds the same energy barrier as in the previous calculation (77), but the prefactor $a^2/D_0(\tilde{\sigma})^{3/2}$ is the Zimm time to diffuse over the first blob: $t_{\text{Zimm}} \propto (\zeta_{\text{first blob}})^3 \propto (\tilde{\sigma})^{-3/2}$.

Appendix 3: Density Relaxation

In order to check that the monolayer is always close to a local equilibrium, i.e., that the composition x is always close to $x_{\text{eq}}(\tilde{\sigma})$, we have solved numerically the relaxation equations (15) and (14). The system of equations is solved by first eliminating the time variable by dividing the two equations and calculating the composition as a function of the density of grafted chains from:

$$\frac{\partial x}{\partial\tilde{\sigma}} = \frac{x^2}{(1-x)\tilde{\sigma}} - \frac{\exp(E - Nx\tilde{\sigma})}{\tilde{\sigma}} \qquad (80)$$

This equation is solved numerically and one gets a curve $x(\tilde{\sigma},N,E)$ (Figure 14). The density equation (14) is then solved by replacing $x(t)$ by $x(\tilde{\sigma}(t),N,E)$. The solution of these exact equations is compared to the approximate solution based on a local equilibrium assumption. The difference between the two results is about 1% as long as $x > 0.75$. The experimental density is not high enough to reach values of x smaller than 0.75. This analysis proves the validity of the local equilibrium approximation $x(t) = x_{\text{eq}}(\tilde{\sigma}(t))$.

References and Notes

(1) Napper, D. H. *Polymer stabilization of colloidal dispersions*; Academic Press: London, 1983; Vol. 1.

(2) Fleer, G. J.; Cohen Stuart, M. A.; Cosgrove, T.; Vincent, B. *Polymer at interfaces*; Chapmann and Hall: London, 1993; Vol. 1.
(3) François, J.; Maître, S.; Rawiso, M.; Beinert, D. S. G.; Isel, F. *Colloids Surf. A* **1996**, *112*, 251−265.
(4) Cao, B. H.; Kim, M. W. *Faraday Discuss.* **1994**, *98*, 245−252.
(5) Alexander, S. *J. Phys. (Fr.)* **1977**, *38*, 983.
(6) Milner, S. T.; Witten, T. A.; Cates, M. E. *Macromolecules* **1988**, *21*, 2610−2619.
(7) Tassin, J. F.; Siemens, R. L.; Tang, W. T. *J. Phys. Chem.* **1989**, *93*, 2106−2111.
(8) Motschmann, H.; Stamm, M. *Macromolecules* **1991**, *24*, 3681−3688.
(9) Johner, A.; Joanny, J. F. *Macromolecules* **1990**, *23*, 5299.
(10) Ligoure, C.; Leibler, L. *J. Phys. Fr.* **1990**, *51*, 1313−1328.
(11) Kopf, A.; Baschnagel, J.; Wittmer, J.; Binder, K. *Macromolecules* **1996**, *29*, 1433−1441.
(12) Wittmer, J.; Johner, A.; Joanny, J. F.; Binder, K. *J. Chem. Phys.* **1994**, *101*, 4379−4390.
(13) Zajac, R.; Chakrabarti, A. *Phys. Rev. E* **1994**, *49*, 3069−3078.
(14) Maître, S. Études des solutions aqueuses de polymères poly(oxyéthylène) modifiés par des extrémités hydrophobes. Thesis, University Louis Pasteur, Strasbourg, France, 1997 (unpublished).
(15) Alami, E.; Rawiso, M.; Isel, F.; Beinert, G.; Binana-Limbele, W.; François, J. Performance with environmental acceptability. *Advances in Hydrophilic Polymers*; American Chemical Society: Washington, DC, 1995; Vol. 248, Chapter 18.
(16) Shuler, R. L.; Zisman, W. A. *J. Phys. Chem.* **1970**, *74*, 1523−1534.
(17) Kawaguchi, M.; Komatsu, S.; Matsuzumi, M.; Takahashi, A. J. *Colloid Interface Sci.* **1984**, *102*, 356−360.
(18) des Cloizeaux, *J. Phys. (Fr.)* **1975**, *36*, 281.
(19) Kuzmenka, D. J.; Granick, S. *Macromolecules* **1988**, *21*, 779−782.
(20) Kuzmenka, D. J.; Granick, S. *Polym. Commun.* **1988**, *29*, 64−66.
(21) Kim, M. W.; Cao, B. H. *Europhys. Lett.* **1993**, *24*, 229−234.
(22) Bekiranov, S.; Bruinsma, R.; Pincus, P. *Europhys. Lett.* **1993**, *24*, 183−188.
(23) Duplantier, B. *J. Stat. Phys.* **1989**, *54*, 581−680. In this paper, γ_I and γ_{II} are calculated at first-order expansion in $\epsilon = 4 - d$ for $d = 3$, and exactly for $d = 2$.
(24) Milner, S. T.; Witten, T. A.; Cates, M. E. *Macromolecules* **1989**, *22*, 853−861.
(25) Nearn, M. R.; Spaull, A. J. B. *Trans. Faraday Soc.* **1969**, *65*, 1785−1793.
(26) van Kampen, N. G. *Stochastic processes in physics and chemistry*; North-Holland Personal Library: Amsterdam, 1992; Vol. 1.
(27) Johner, A.; Joanny, J. F. *J. Chem. Phys.* **1993**, *98*, 1647−1658.
(28) Abramovitz, M.; Stegen, I. *Handbook of Mathematical Functions*; Dover: New York, 1972.

MA971665X